Available online at www.sciencedirect.com
SCIENCE DIRECT®
PERGAMON
International Journal of Heat and Mass Transfer 47 (2004) 1–10
International Journal of HEAT and MASS TRANSFER
www.elsevier.com/locate/ijhmt

A one-dimensional numerical study of the salt diffusion in a salinity-gradient solar pond

Celestino Angeli [a], Erminia Leonardi [b,*]

[a] Dipartimento di Chimica, Università di Ferrara, Via Borsari 46, I-44100 Ferrara, Italy
[b] CRS4, Center for Advanced Studies, Research and Development in Sardinia, Parco Scientifico e Tecnologico, Polaris, Edificio 1, 09010 Pula, CA, Italy

Received 3 April 2003; received in revised form 15 July 2003

Abstract

A one-dimensional transient mathematical model is used for the study of the salt diffusion and stability of the density gradient in a solar pond. A finite difference method with a diffusion coefficient dependent on both temperature and salt concentration is used to solve the salt diffusion equation. On the basis of simple considerations we analyze the influence of the salinity-gradient thickness on the useful energy which can be withdrawn from the bottom layer of the solar pond. Finally some considerations on the effect of the velocity of injected brine in rising solar ponds are presented, making use of the Rayleigh analysis of the small perturbations in order to study the stability of the system.

Keywords: Solar pond; Salt diffusion; Finite difference 1D numerical methods; Rayleigh analysis

1. Introduction

A solar pond is a simple and low cost mean to collect and store solar energy in the form of hot high-density salt water. It consists of three main layers (see Fig. 1). The top layer (upper convective zone, UCZ) is cold, close to the atmospheric temperature, and has low salt concentration. The bottom layer (lower convective zone, LCZ) is hot, 70–100 °C, and very salty (typically, close to saturation). These two layers are characterized by almost homogeneous temperature and concentration due to convection. Separating these two layers is the important gradient zone (non-convective zone, NCZ), where salt content increases with depth. Water in this layer cannot rise because the water above it has less salt content and is therefore lighter. Similarly, water cannot fall because the water below it has a higher salt content and is heavier. Therefore convective motions are hindered and heat transfer from the hot LCZ to the cold UCZ can only happens through conduction. Given the low thermal conductivity of water, the NCZ layer acts as a transparent insulator, permitting sunlight to be trapped in the hot bottom layer, from which useful heat is withdrawn.

Despite the simplicity of its working mechanism, the large number of physical phenomena involved in its operation makes the full description of the system a very difficult problem from both the physical and the mathematical points of view. In fact, although the physics of each phenomenon is quite well known, the coupling between the phenomena needs further investigations.

A lot of theoretical studies have concentrated on modelling the heat and salt diffusion within the solar pond for predicting its stability and performance. Weinberger [1] was the first to give a mathematical formulation of the behavior of a salinity-gradient solar pond. He identified and analyzed many important physical processes for the stability of the salinity-gradient layer, such as the absorption of the solar radiation by the brine solution, the losses to the atmosphere and

* Corresponding author. Tel.: +39-070-9250328; fax: +39-070-9250216.
E-mail address: ermy@crs4.it (E. Leonardi).

0017-9310/$ - see front matter
doi:10.1016/S0017-9310(03)00410-1

Nomenclature

a, b	fitting parameters, dimensionless
c	salt concentration, $\mathrm{kg\,m^{-3}}$
c_p	heat capacity at constant pressure, $\mathrm{J\,kg^{-1}\,°C^{-1}}$
D	salt diffusivity, $\mathrm{m^2\,s^{-1}}$
H	solar pond total thickness, m
$\vec{J}$	mass flux, $\mathrm{kg\,m^{-2}\,s^{-1}}$
k	thermal conductivity, $\mathrm{W\,m^{-1}\,°C^{-1}}$
K_T	thermal diffusivity, $\mathrm{m^2\,s^{-1}}$
LCZ	lower convective zone
NCZ	non-convective zone
$\dot{q}$	heat generated per unit time and volume, $\mathrm{W\,m^{-3}}$
$\overline{Q}$	useful heat withdrawn from the LCZ per unit time and area, $\mathrm{W\,m^{-2}}$
Q_g	heat losses from the LCZ to the ground per unit time and area, $\mathrm{W\,m^{-2}}$
$\overline{Q}_i$	ideal value of $\overline{Q}$, $\mathrm{W\,m^{-2}}$
S	salinity, %
T	temperature, °C
T_L	temperature in the LCZ, °C
T_U	temperature in the UCZ, °C
UCZ	upper convective zone
$\vec{v}$	velocity, $\mathrm{m\,s^{-1}}$
W	solar power density, $\mathrm{W\,m^{-2}}$
W_0	solar power density at the water surface, $\mathrm{W\,m^{-2}}$
z	solar pond height, measured from the bottom ($z = H - Z$), m
Z	solar pond depth, measured from the surface, m
Z_L	solar pond depth measured at the LCZ–NCZ boundary, m
Z_U	solar pond depth measured at the UCZ–NCZ boundary, m

Greek symbols

θ_t	refraction angle, radian
ν	kinematic viscosity, $\mathrm{m^2\,s^{-1}}$
ρ	density, $\mathrm{kg\,m^{-3}}$

Superscripts

$\vec{x}$	vector variable
$\dot{x}$	time derivative

to the ground, and the double-diffusion effect. The analytical solution of the partial differential equation for the transient temperature distribution was obtained by superimposing the effects of the radiation absorption at the surface, in the body of the water and at the bottom. Meyer [2] has developed a numerical model to predict the time-dependent behavior of the interface between the convecting and the non-convecting regions of the solar pond. The model utilizes the empirical correlation that describes the heat and the salt fluxes across the interfaces of the pond regions. Panahi et al. [3] developed a one-dimensional model to simulate the dynamic performance of the salinity-gradient solar pond using a finite-element technique. The model takes account of energy flux as well as the variation of brine densities as functions of temperature and salt concentration in order to examine various pond stability criteria. Rubin and Benedict [4] used a finite-difference implicit model to solve the equations that relate the various parameters involved in the solar pond model. These are the solar radiation input, diffusion and dispersion of the heat within the pond as well as the withdrawal of heat from layers within the pond. Beniwal and Singh [5] modelled the salt-gradient solar pond as a steady-state flat plate collector. This model was used to optimize the values for the geometrical and operational parameters of the solar pond. Giestas et al. [6] have given important contributions to clarify the effect on the solar pond stability of non-constant thermal and molecular diffusion coefficients. Jayaprakash and Perumal [7] have performed an experimental study on the stability of an unsustained solar pond, comparing the monitored density profile with a one-dimensional model where the salt diffusivity is a linear function of the temperature. Alagao [8] has proposed a one-dimensional model to simulate a closed-cycle solar pond, by using both analytical and finite difference explicit models, with a salt diffusivity varying linearly with the temperature.

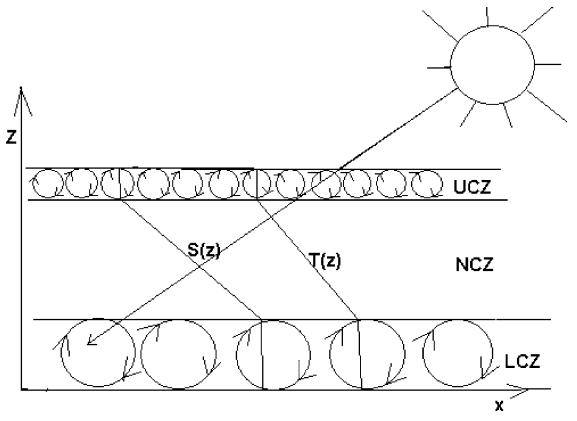

Fig. 1. Schematic of a solar pond.

As said before, many physical phenomena are relevant for a solar pond and they are often coupled. In this

sense it would be desirable to treat simultaneously the heat and the salt diffusion and, if possible, the convective motions in the convective zones. This approach is out of the scope of this paper due to its complexity and we focus our attention to specific aspects of the solar pond behavior. In particular we do not explicitly treat the heat diffusion problem and its coupling with mass diffusion.

The aim of the present paper is to predict the solar pond stability and performance by calculating the optimum salinity-gradient thickness and its transient behavior, taking account of the seasonal changes of both solar radiation and solar pond temperature. A one-dimensional finite-difference semi-implicit model is used, the transient behavior of a solar pond with brine injection is simulated, and instability development is analyzed. The remainder of the paper is organized as follows: in the next section the thickness of the salinity-gradient layer which maximize the useful energy is evaluated on the basis of a simplified model and in Section 3 the salt diffusion process is analyzed using a finite difference numerical approach.

2. Influence of the NCZ thickness on the energy efficiency

The efficiency of a solar pond is strongly governed from the NCZ structure. We stress that the NCZ layer is unstable from both a dynamical and a thermodynamical point of view. Indeed natural and forced convection in the UCZ and in the LCZ lead to an erosion at the boundaries of the NCZ [9,10] and the salt diffusion tends to homogenize the salt concentration thus reducing the NCZ thickness. For these reasons operative interventions must be planned in order to systematically adjust the salinity-gradient profile. The number and the nature of such interventions depend obviously from the NCZ characteristics (among which the thickness) but we shall not consider this aspect in this paper. On the other hand a crucial requirement concerns the useful energy which must be maximized: the subject of this section is to derive the influence of the NCZ thickness on the energy available in the LCZ by using a simple model.

It is clear that only a fraction of the solar energy reaching the solar pond surface is available in the LCZ. Indeed, part of the radiation is reflected at the surface and part is absorbed by the water body of the UCZ and NCZ before reaching the LCZ. Moreover, the solar energy which reaches the LCZ is not fully available due to the energy released to the ground and to the NCZ through conduction.

Both the fraction of the solar power entering the LCZ and the energy lost from the LCZ through conduction versus the NCZ depends on the NCZ thickness which should therefore be optimized. The energy loss to the ground is quite complex to estimate, but we can reasonably suppose that it is constant if the LCZ temperature is maintained constant. This assumption strongly simplify the following derivation and it is justified from the fact that in actual solar ponds there is an energy withdrawal from the LCZ. We assume that such energy withdrawal maintains the LCZ temperature constant with respect to time and we search for the maximum value of the withdrawn energy.

The equation governing the diffusion of heat in a conductor states

$$\rho c_p \frac{\partial T}{\partial t} = \dot{q} + \frac{\partial}{\partial Z}\left(k \frac{\partial T}{\partial Z}\right) \tag{1}$$

where ρ ($\mathrm{kg\,m^{-3}}$) is the density, c_p ($\mathrm{J\,kg^{-1}\,°C^{-1}}$) is the heat capacity at constant pressure, $\dot{q}$ ($\mathrm{W\,m^{-3}}$) is the heat generated per unit time and volume, k ($\mathrm{W\,m^{-1}\,°C^{-1}}$) is the thermal conductivity.

In our case the term $\dot{q}$ is the solar energy absorbed from the water per unit time and volume, that is

$$\dot{q} = -\frac{\partial W}{\partial Z} \tag{2}$$

where $W(Z)$ ($\mathrm{W\,m^{-2}}$) is the solar power density at the depth Z measured from the water surface.

The solar radiation decay in water can be expressed with a good approximation [11] as

$$\frac{W(Z)}{W_0} = a - b \ln\left(\frac{Z}{\cos\theta_t}\right) \tag{3}$$

where W_0 ($\mathrm{W\,m^{-2}}$) is the solar power density which penetrates the water surface ($Z = 0$), θ_t is the refraction angle and $a = 0.4415$ and $b = 0.094085$ are obtained by a fitting procedure [12] of the experimental water absorption coefficient in the depth range from 0 to 3.5 m.

Therefore

$$\dot{q} = -\frac{\partial}{\partial Z}\left\{W_0\left[a - b\ln\left(\frac{Z}{\cos\theta_t}\right)\right]\right\} = \frac{W_0 b}{Z} \tag{4}$$

Assuming the temperature constant with respect to time in Eq. (1) and k constant with respect to Z (that is, temperature and salinity independent), the temperature profile within the salinity-gradient layer is obtained by successive integrations of the equation

$$\frac{\partial^2 T}{\partial Z^2} = -\frac{W_0 b}{kZ} \tag{5}$$

Therefore we have

$$\frac{\partial T}{\partial Z} = -\frac{W_0 b}{k}\ln(Z) + C_1 \tag{6}$$

$$T(Z) = -\frac{W_0 b}{k}[Z\ln(Z) - Z] + C_1 Z + C_2 \tag{7}$$

The two constants C_1 and C_2 are given by

$$C_1 = \frac{T_L - T_U}{Z_L - Z_U} - \frac{W_0 b}{k}\left[1 - \frac{Z_U \ln(Z_U) - Z_L \ln(Z_L)}{Z_U - Z_L}\right] \quad (8)$$

$$C_2 = T_L + \frac{W_0 b}{k}[Z_L \ln(Z_L) - Z_L] - C_1 Z_L \quad (9)$$

where Z_L and Z_U are the values of Z at the lower and upper boundaries of the NCZ layer, respectively and T_L and T_U are the corresponding temperatures. Moreover, due to convection, we also assume that T_L and T_U are the (homogeneous) temperatures of the LCZ and UCZ, respectively.

In the following (Section 3.2) we shall use the temperature profile here obtained for the study of the time evolution of the salinity gradient of a solar pond. In order to approach an actual description of the system we shall consider a seasonal change of the LCZ and UCZ temperatures. It can be argued that the use of LCZ and UCZ temperatures variable in time, which implies a time-dependent temperature profile, is in contrast with the derivation here developed in which the temperature is assumed to be constant in time. Actually one can use the fact that the seasonal evolution of the solar power density and of the atmospheric temperature, which induce the modification of the LCZ and UCZ temperatures, develops in a time scale much longer than the time scale in which the temperature profile adapts itself to the new values of T_U and T_L. In practice one can imagine that the temperature profile is instantaneously defined by the varying LCZ and UCZ temperatures. With this assumption our approach remains correct.

The heat which can be extracted from the LCZ, $\overline{Q}$, can be expressed in terms of an energy balance between the solar energy reaching the LCZ (obtained from Eq. (3)) and the conduction heat losses to the NCZ and to the ground, Q_g

$$\begin{aligned}\overline{Q} &= W_0\left[a - b\ln\left(\frac{Z_L}{\cos\theta_t}\right)\right] - k\left.\frac{\partial T}{\partial Z}\right|_{Z_L} - Q_g \\ &= W_0\left[a - b\ln\left(\frac{Z_L}{\cos\theta_t}\right)\right] - k\left[-\frac{W_0 b}{k}\ln(Z_L) + C_1\right] - Q_g\end{aligned} \quad (10)$$

The optimum thickness of the NCZ is given imposing

$$\frac{\partial \overline{Q}}{\partial Z_L} = 0 \quad (11)$$

and noting that Q_g does not depend on Z_L within our model, one gets

$$T_L - T_U = -\frac{W_0 b}{k}\left\{\left[1 + \ln\left(\frac{Z_L}{Z_U}\right)\right]Z_U - Z_L\right\} \quad (12)$$

The second derivatives of $\overline{Q}$ with respect to Z_L computed for the value of Z_L which satisfies Eq. (11)

$$\frac{\partial^2 \overline{Q}}{\partial Z_L^2} = \frac{W_0 b}{(Z_L - Z_U)^2}\left[\frac{Z_U}{Z_L} - 1\right] \quad (13)$$

confirms that the condition in Eq. (12) is obtained for a maximum of $\overline{Q}$. Indeed one can easily verify that the right hand side of Eq. (13) is negative ($Z_U < Z_L$).

By numerically solving Eq. (12) with respect to Z_L and replacing its value in Eq. (10) we find the maximum useful heat available in the LCZ. Actually in order to know $\overline{Q}$ we need to estimate Q_g which depends on many constructive characteristics (but not on the NCZ thickness within our model). We therefore introduce the quantity $\overline{Q}_i = \overline{Q} + Q_g$ which is the upper limit for the useful energy and it is equal to $\overline{Q}$ for an ideal perfectly insulated solar pond bottom ($Q_g = 0$).

Fig. 2 shows the dependence of the optimum NCZ thickness and ideal heat efficiency, $\eta_i = \overline{Q}_i / W_0$, from the LCZ temperature. In this case we have assumed $W_0 = 300\ \mathrm{W\,m^{-2}}$, $T_U = 20\ ^\circ\mathrm{C}$, $Z_U = 0.5$ m and $\cos\theta_t$ has been replaced in the equations by its time averaged value $\langle(\cos\theta_t)^{-1}\rangle = 1.16$, which are reasonable parameters for a solar pond located at the latitude of 39°N during the summer period (the location of southern Sardinia, Italy). From Fig. 2 we note that the ideal heat efficiency is a decreasing function of the LCZ temperature, due to the fact that the conduction heat losses from the LCZ to the NCZ increases with the LCZ temperature.

The ideal heat efficiency is lower during the winter period, when typical solar radiation of about 140 $\mathrm{W\,m^{-2}}$

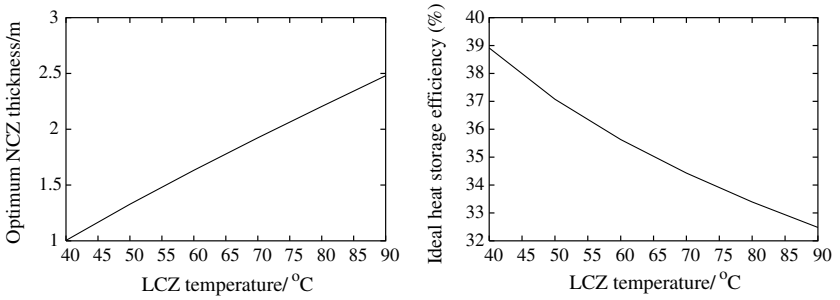

Fig. 2. Dependence of the optimum NCZ thickness (left) and ideal heat storage efficiency (right) from the LCZ temperature (T_U = 20 °C).

(at 39°N) is available, and UCZ and LCZ temperatures are about 10 and 70 °C, respectively. In this case, if a solar pond is constructed to maximize the solar energy capture during the summer (when the LCZ temperature can easily reach about 90 °C, and, therefore, the NCZ thickness is of about 2.5 m), in winter a heat storage efficiency of about 26% should be attained, which is about 4% less than its maximum obtainable value (which should correspond to a NCZ thickness of about 4 m).

3. The salt diffusion within the solar pond

As mentioned in the previous section, the crucial aspect of a solar pond operation is the NCZ stability (convective motions are hindered), which is ensured by a strong enough salinity gradient. Obviously the salinity gradient is unstable from a thermodynamical point of view, given that diffusion tends to homogenize the salt concentration.

The maintenance of the salinity profile within the NCZ can be obtained by addition of salt in the LCZ and flushing with fresh water or low salinity water at the UCZ (this is done in order to take into account both salt diffusion from the NCZ and evaporative water losses at the surface). These interventions must be planned by monitoring the modifications of the salinity gradient. Therefore the dynamic of the salt diffusion is a key phenomenon to study and to keep under control.

In this section we present some considerations on the salt diffusion in the solar pond, its time-scale and temperature dependence.

3.1. The mathematical model

The principle of mass transfer for the solute results in an equation of the form:

$$\frac{\partial c}{\partial t} = -\vec{\nabla}\cdot\vec{J} = -\vec{\nabla}\cdot(\vec{v}c - D\vec{\nabla}c), \tag{14}$$

where $\vec{J}$ is the mass flux, $\vec{v}$ is the velocity, c is the solute concentration, D is the diffusion coefficient and the operator $\vec{\nabla}\cdot$ is simply $\frac{\partial}{\partial z}\cdot$ in the present model.

In the case of a rising solar pond, v is the rise velocity of the NCZ, positive upward, and it is constant with respect to time and space. In a first approximation, a solar pond can be thought as composed of horizontal layers of infinitesimal thickness, which are homogeneous in concentration. Following this approximation, the process of salt diffusion can be studied using a one-dimensional approach. Therefore we have used a one-dimensional (1D) finite difference scheme to solve the above equation. The concentration $c(z,t)$ is computed on a regular grid of points in z ($\{z_1, z_2, \ldots, z_{n_z}\}$, $z_{i+1} - z_i = \Delta z$) and t ($\{t_1, t_2, \ldots, t_{n_t}\}$, $t_{i+1} - t_i = \Delta t$). For the sake of simplicity we use the compact formalism $c_{i,j}$ for $c(z_i, t_j)$. We have used the second-order accurate in time Crank–Nicholson scheme with a position dependent diffusion coefficient [13]:

$$\begin{aligned}\frac{c_{i,j} - c_{i,j-1}}{\Delta t} = &-v\frac{(c_{i+1,j} - c_{i-1,j}) + (c_{i+1,j-1} - c_{i-1,j-1})}{4\Delta z} \\ &+ \frac{1}{2(\Delta z)^2}\{D_{i+\frac{1}{2}}[(c_{i+1,j} - c_{i,j}) \\ &+ (c_{i+1,j-1} - c_{i,j-1})] + D_{i-\frac{1}{2}}[(c_{i-1,j} - c_{i,j}) \\ &+ (c_{i-1,j-1} - c_{i,j-1})]\}\end{aligned} \tag{15}$$

where

$$D_{i+\frac{1}{2}} = \frac{D(z_{i+1}) + D(z_i)}{2} \tag{16}$$

$$D_{i-\frac{1}{2}} = \frac{D(z_{i-1}) + D(z_i)}{2} \tag{17}$$

Eq. (15) can be rewritten in the form of a system of linear equations (one set for each time t_j)

$$\begin{aligned}&\left(\beta - \alpha_{i+\frac{1}{2}}\right)c_{i+1,j} + \left(1 + \alpha_{i+\frac{1}{2}} + \alpha_{i-\frac{1}{2}}\right)c_{i,j} \\ &\quad - \left(\beta + \alpha_{i-\frac{1}{2}}\right)c_{i-1,j} = B_{i,j}\end{aligned} \tag{18}$$

where

$$\beta = \frac{v\Delta t}{4\Delta z} \tag{19}$$

$$\alpha_{i+\frac{1}{2}} = \frac{D_{i+\frac{1}{2}}\Delta t}{2(\Delta z)^2} \tag{20}$$

$$\alpha_{i-\frac{1}{2}} = \frac{D_{i-\frac{1}{2}}\Delta t}{2(\Delta z)^2} \tag{21}$$

and

$$\begin{aligned}B_{i,j} = &-\frac{v\Delta t}{4\Delta z}(c_{i+1,j-1} - c_{i-1,j-1}) + \alpha_{i+\frac{1}{2}}(c_{i+1,j-1} - c_{i,j-1}) \\ &+ \alpha_{i-\frac{1}{2}}(c_{i-1,j-1} - c_{i,j-1}) + c_{i,j-1}\end{aligned} \tag{22}$$

The system of linear equations (18) can be written in the matrix form

$$\mathbf{A}\mathbf{C}_j = \mathbf{B}_j \quad \forall j = 2, n_t \tag{23}$$

and it can be easily solved, once the initial ($c_{i,0}$, for all i) and boundary conditions ($c_{1,j}$ and $c_{n_z,j}$ at each time t_j) are imposed, by using standard mathematical libraries such as for instance the LAPACK ones [14]. We note, in passing, that our scheme, being a semi-implicit method, is stable for any Δt [13], therefore we do not have restrictions on the time step size apart from those imposed by the required accuracy.

Following Alagao [8], the two boundary conditions for the NCZ do not depend on time and are given by

(1) at the bottom: $J = vc^*$, where c^* and v are the concentration and the velocity of the injected brine, respectively,
(2) at the top: $c = c_U$, where c_U is the concentration of the flushed UCZ.

Once the diffusion problem has been solved, thus obtaining the value for $c_{i,j}$, the following properties can be obtained:

- the flux, $J_{i,j}$ ($\mathrm{kg\,m^{-2}\,day^{-1}}$), at any point z_i, t_j
- the density, $\rho_{i,j}$ ($\mathrm{kg\,m^{-3}}$), at any point z_i, t_j: it is a function of the temperature T and of the salinity S ($\mathrm{g\,kg^{-1}}$). In the case of a NaCl aqueous solution ρ is given by [15]:

$$\rho(z,t) = 1000 \times \left\{1 - \frac{T+a}{b\times(T+c)} \times (T-d)^2\right\} + e(T)\times S + f(T)\times S^{\frac{3}{2}} + g\times S^2 \tag{24}$$

where $a = 288.9414$, $b = 508929.2$, $c = 68.12963$, $d = 3.9863$, $g = 4.8314\times10^{-4}$ and

$$e(T) = 8.24493\times10^{-1} - 4.0899\times10^{-3}\times T + 7.6438\times10^{-5}\times T^2 - 8.2467\times10^{-7}\times T^3 + 5.3675\times10^{-9}\times T^4$$

$$f(T) = -5.724\times10^{-3} + 1.0227\times10^{-4}\times T - 1.6546\times10^{-6}\times T^2$$

We do not have direct access to the salinity because it is, in its turn, a function of the concentration and of the density

$$S(z,t) = \frac{c(z,t)}{\rho(z,t)} \tag{25}$$

Therefore the calculation of $\rho_{i,j}$ has been implemented in an iterative scheme: we consider first $S_{i,j} = c_{i,j}$, then compute $\rho_{i,j}$ using Eq. (24) and finally compute $S_{i,j}$ using Eq. (25). The process is repeated until the variation of ρ between two successive steps is lower than a certain threshold. The salinity function $S(z,t)$ is therefore another output of the program.

Two different expressions for the diffusion coefficient D have been implemented in our code: the first is [16,17]

$$D_i = D_0 \times [1 + 0.029(T_i - 20)] \tag{26}$$

which gives the dependence of the diffusivity coefficient on the temperature (°C) for a NaCl aqueous solution. D_0 is equal to 1.39×10^{-9} in $\mathrm{m^2\,s^{-1}}$ or 1.20×10^{-4} in $\mathrm{m^2\,day^{-1}}$.

A more precise expression, in which also the dependence on the salinity is considered, is obtained by a least square fit to the International Critical Tables for a range of temperature between 5 and 100 °C and for a salinity range between 0% and 20% [6]

$$D_{i,j} = (8.16 + 0.255T_i + 0.00254T_i^2 - 0.28S_{i,j} + 0.0147S_{i,j}^2)\times10^{-10} \tag{27}$$

where S is the salinity in wt% ($S = c/\rho\times100$) and $D_{i,j}$ is in $\mathrm{m^2\,s^{-1}}$. It is clear that Eq. (27) for D makes the study of mass diffusion a complex non-linear problem. We have implemented two alternative solutions in order to keep the approach simple:

(1) $D_{i,j}$ is computed using the salinity $S_{i,j-1}$ at time t_{j-1}, which is a very good approximation, given that D has a small dependence on S and that S (or c) changes very slowly from one time step to the next one;
(2) for each time step t_j the concentration c is computed iteratively, each step consisting in the computation of D using the values of S obtained at the previous step and recomputing c. For the first step the values of D are obtained following the approximation described in point 1. The iterative approach is stopped when a convergence criterion is satisfied.

Obviously the steady state solution is not affected by which of the two methods is used.

The temperature profile within the solar pond is computed from Eq. (1). Moreover, since diffusion is a slow process, the transient should take into account the seasonal changes of the solar radiation density and of the average LCZ and UCZ temperatures. Both solar radiation and LCZ and UCZ temperatures are parameters which depend on latitude, weather and ground characteristics, therefore these informations should be obtained from experimental measurements and treated as input data for the numerical code.

The stability of a solar pond warmed by solar radiation is maintained by means of a sufficiently steep salt concentration gradient. From the Rayleigh analysis of the small perturbations to which all natural systems are susceptible [16] it comes out that the salt gradient required for maintaining the stability is given by

$$\mathscr{F} \overset{\text{def}}{=} \frac{\partial c}{\partial z} + \frac{(v+K_T)\left(\frac{\partial\rho}{\partial T}\right)\left(\frac{\partial T}{\partial z}\right)}{(v+D)\left(\frac{\partial\rho}{\partial c}\right)} \leqslant 0 \tag{28}$$

where v is the kinematic viscosity (in $\mathrm{m^2\,s^{-1}}$), K_T is the thermal diffusivity (in $\mathrm{m^2\,s^{-1}}$) and we have introduced the instability function $\mathscr{F}$ (for $\mathscr{F} \leqslant 0$ the system is stable with respect to small perturbations). The derivatives $\frac{\partial\rho}{\partial T}$ and $\frac{\partial\rho}{\partial c}$ $\left(= \frac{1}{\rho}\frac{\partial\rho}{\partial S}\right)$ are obtained from Eq. (24), while $\frac{\partial T}{\partial z}$ is given by Eq. (6). Let us note that with respect to Ref. [16] the direction of the inequality is inverted due to the different definition of z.

In the LCZ and UCZ, convective motions develop on a time scale much shorter than the diffusive motions, maintaining their temperature and concentration homogeneous at any time step. Therefore, we have implemented the possibility of averaging the concentration in the LCZ and UCZ, after the solution of the diffusion equation at each time step.

3.2. Discussion of the simulation results

In this paper we discuss the salt diffusion, neglecting the thermodiffusion effect, which is the salt tendency to migrate under the effect of a temperature gradient (Soret effect).

At this level, our results are approximated, but, nevertheless, they give an idea of the time-scale of the salt diffusion and of the onset of the instabilities within the solar pond.

As a first application we have considered the influence of the diffusion coefficient profile on the steady state concentration. In order to compare our results with those of Alagao [8], we have considered a NCZ thickness of 1.0 m. The initial NaCl concentration ($\mathrm{kg\,m^{-3}}$) is assumed to be a linear function of the depth, ranging from 200 at the bottom of the NCZ to 40 at its upper surface. The brine is injected at the bottom of the NCZ at a velocity, v, of 2.778×10^{-4} m day^{-1} and it has a NaCl concentration, c^*, of 311.25 $\mathrm{kg\,m^{-3}}$. We focus our attention on the NCZ layer, and therefore we suppose the LCZ and UCZ to have a zero thickness. The salt diffusion is computed by discretization of the computational domain with $\Delta z = 0.01$ m, and $\Delta t = 1.0$ day. First of all, we have tested our code performing a calculation in which the salt diffusion coefficient is taken from Ref. [8]: the analytical steady-state concentration profile found by Alagao is obtained after a transient of 15 years. For comparison we report in Fig. 3 the salt diffusion coefficient computed from Eqs. (26) and (27) and from the expression used by Alagao [8].

From Fig. 3 one notes that the three curves, although being quite similar in the upper part of the NCZ, partially differ in the salty and worm bottom part of the NCZ. We have therefore chosen to use in the following Eq. (27) to compute D.

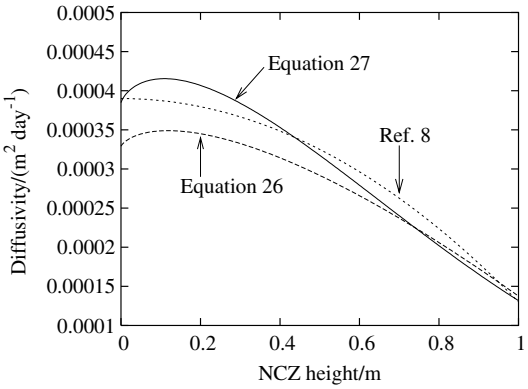

Fig. 3. Comparison of the salt diffusion coefficient computed with three different approximate expressions, as a function of the NCZ height for a solar pond as defined in Ref. [8] ($T_L = 80$ °C, $T_U = 25$ °C, NCZ thickness of 1 m). The salt concentration varies linearly from 200 $\mathrm{kg\,m^{-3}}$ at $z = 0$ m to 40 $\mathrm{kg\,m^{-3}}$ at $z = 1$ m. When the salt diffusion coefficient is obtained from Eq. (27) we use the initial salinity profile which varies almost linearly.

We want now to study the transient behavior and the effect of the injected brine for a solar pond located in a Mediterranean country. The temperature and solar power density are supposed to follow the time evolution of Fig. 4 which are reasonable choices for this area.

The NCZ thickness is chosen to be the optimum thickness for the summer period when a solar power density of 300 $\mathrm{W\,m^{-2}}$ and a LCZ temperature of 90 °C are reasonable values. As found in Section 2 (Fig. 2), the optimum NCZ thickness for such parameters is 2.5 m. All the other parameters are those used in the previous simulation for the comparison with the results of Ref. [8].

The time evolution for a transient of 40 years of the concentration computed at four values of the NCZ height ($z = 0.5$, 1.0, 1.5, 2.0 m) is reported in Fig. 5.

From this figure one senses that the periodicity of the UCZ and LCZ temperatures and of the solar power

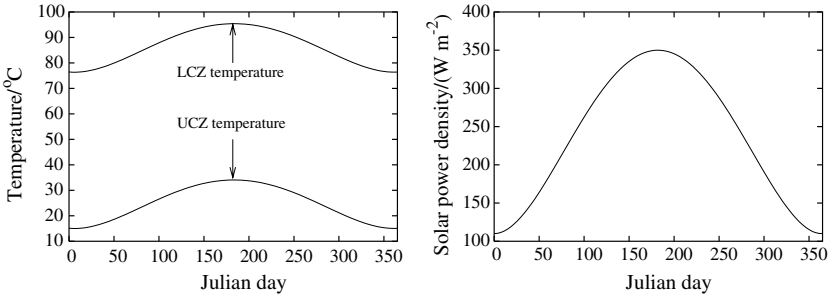

Fig. 4. Variation of the LCZ and UCZ temperature (left) and solar power density (right) during the Julian year.

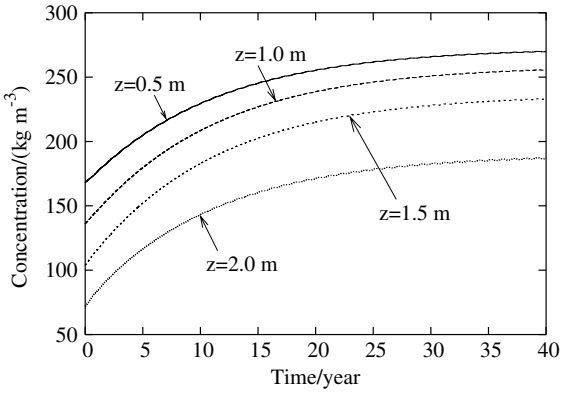

Fig. 5. Time evolution of the concentration computed at four values of the NCZ height ($z = 0.5$, 1.0, 1.5, 2.0 m) for a solar pond with a NCZ thickness of 2.5 m, a brine injection velocity and concentration of 2.778×10^{-4} m day^{-1} and 311.25 kg m^{-3}, respectively. The initial salt concentration varies linearly from 200 kg m^{-3} at $z = 0$ m to 40 kg m^{-3} at $z = 2.5$ m.

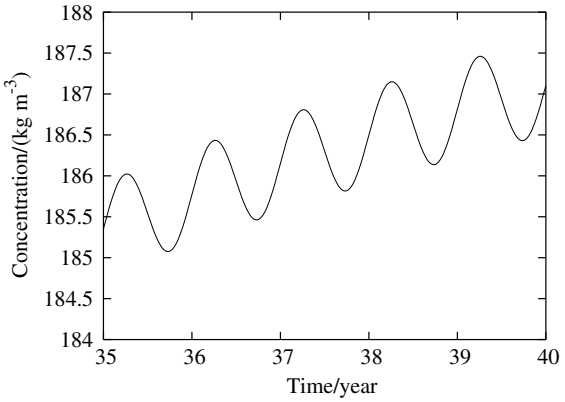

Fig. 6. Zoom of the $z = 2$ m curve of Fig. 5 in the time interval 35–40 years.

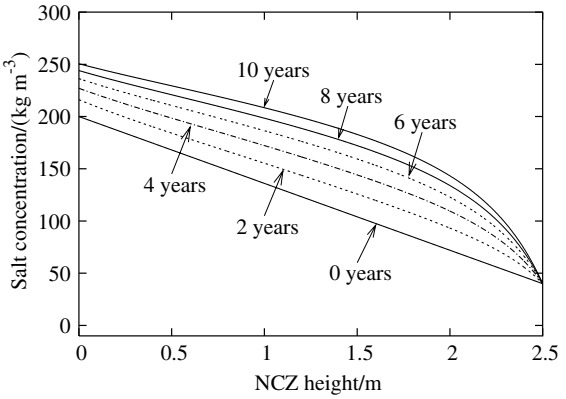

Fig. 7. Salt concentration profile at six different times ($t = 0$, 2, 4, 6, 8, 10 years). The solar pond parameters are the same as in Fig. 5.

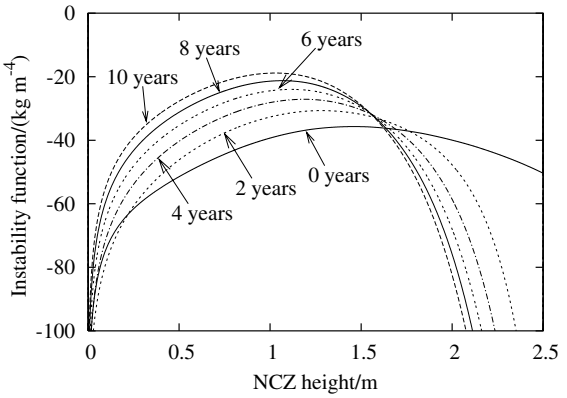

Fig. 8. Instability function, $\mathscr{F}$, profile at six different times ($t = 0$, 2, 4, 6, 8, 10 years). The solar pond parameters are the same as in Fig. 5.

density is reflected on the evolution of the concentration. Therefore the system does not reach a true steady-state but rather a "pseudo steady-state" where the concentration periodically oscillates around a constant value. The amplitude of the oscillation is small with respect to the changes of the concentration with the NCZ height. The oscillation are less relevant at the beginning of the time evolution and becomes significant for long times, when the "pseudo steady-state" is reached, as shown in Fig. 6 where a zoom of the final part of the $z = 2.0$ m curve is plotted.

In Figs. 7 and 8 we report the transient behavior of the concentration profile and of the instability function (see Eq. (28)).

From Fig. 8 one can note that the instability function always remains below zero, thus guaranteeing that the rising of convective motion is hindered. It is clear that this is due to a large enough velocity of the injected saturated brine. Indeed, in the limiting case of a zero velocity, the steady-state (in this case no oscillating behavior occurs for large times) has a constant concentration and the system results obviously unstable. We have found that with a velocity of the injected brine $v = 5.5 \times 10^{-5}$ m day^{-1} instability appears at the quasi-steady state while for lower values of v instabilities develop at finite time. For instance with $v = 3.0 \times 10^{-5}$ m day^{-1} the instability function becomes greater than zero in an interval around $z = 1$ m after eight years.

Finally, we explore the influence of the NCZ thickness on the effects considered above. The time evolution of the salt concentration for four values of the NCZ height ($z = 0.2$, 0.4, 0.6, 0.8 m) and with the same solar pond parameters used in the case plotted in Fig. 5, but

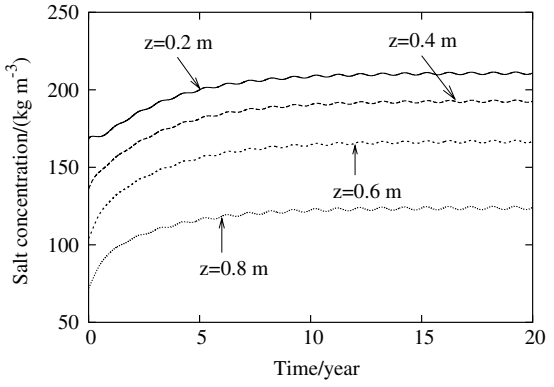

Fig. 9. Time evolution of the concentration computed at four values of the NCZ height ($z = 0.2$, 0.4, 0.6, 0.8 m) for a solar pond with a NCZ thickness of 1.0 m, a brine injection velocity and concentration of 2.778×10^{-4} m day^{-1} and 311.25 kg m^{-3}, respectively. The initial salt concentration varies linearly from 200 kg m^{-3} at $z = 0$ m to 40 kg m^{-3} at $z = 1.0$ m.

with a NCZ thickness of 1 m are reported in Fig. 9. Given that in this case the quasi-steady state is reached faster than with the NCZ thickness of 2.5 m, the time of the simulation reported in Fig. 9 has been reduced to 20 years. One can note that in this case the amplitude of the oscillations at the quasi-steady state is greater than in the previous case and they appear since the beginning of the simulation.

From the analysis of the instability function it results that the stability of the system is improved with respect to the case with a NCZ thickness of 2.5 m and therefore lower values of v are allowed without the appearance of instabilities.

4. Conclusions

In this study, after some preliminary considerations which justifies the typical thickness of the salinity-gradient layer, a 1D mathematical model of the salt diffusion within the solar pond has been presented and discussed. The equation obtained for the model has been solved numerically by using the finite difference method. In order to simulate a transient, we have assumed arbitrary but reasonable functions to describe the fluctuations of both the temperatures of the LCZ and UCZ and the solar power density during the year. In a quantitative study, these parameters should be experimental data, being strongly dependent on the geographical location of the solar pond, and the thermal properties of the ground.

The Rayleigh analysis has been used to follow the onset of convection within the salinity-gradient layer. We have confirmed that although the salt diffusion is a very slow process, to make the solar pond operative for many years (typically, 15–20 years), one must operate in order to compensate the variation of the salt concentrations at the NCZ boundaries, by adding saturated brine in the LCZ and flushing the UCZ.

Acknowledgements

The authors thank Bruno D'Aguanno for useful discussions and suggestions. This work has been carried out with the financial support of the "Regione Autonoma della Sardegna".

References

[1] H. Weinberger, The physics of solar pond, Solar Energy 8 (1964) 45.
[2] K.A. Meyer, Numerical model for describing the layer behavior in salt-gradient solar pond, J. Solar Energy Eng., ASME Trans. 105 (1983) 341.
[3] Z. Panahi, J.C. Batty, J.P. Riley, Numerical simulation of the performance of a salt-gradient solar pond, J. Solar Energy Eng., ASME Trans. 105 (1983) 369.
[4] H. Rubin, B.A. Benedict, Modelling the performance of a solar pond as a source of thermal energy, Solar Energy 32 (1984) 771.
[5] R.S. Beniwal, R. Singh, Calculation of the thermal efficiency of salt gradient solar ponds, Heat Recovery Syst. CHP 7 (1987) 497.
[6] M. Giestas, A. Joyce, H. Pina, The influence of non-constant diffusivities on solar ponds stability, Int. J. Heat Mass Transfer 18 (1997) 4379.
[7] R. Jayaprakash, K. Perumal, The stability of an unsustained salt gradient solar pond, Renewable Energy 4 (1998) 543.
[8] F.B. Alagao, Simulation of the transient behavior of a closed-cycle salt-gradient solar pond, Solar Energy 5 (1996) 245.
[9] M.J. Witte, T.A. Newell, A thermal burst model for the prediction of erosion and growth rates of a diffusion interface, in: National Heat Transfer Conference, ASME paper 85-HT-31, Denver, CO, 1985.
[10] F. Zangrando, Hydrodynamics of salt-gradient solar ponds, Solar Energy 46 (1991) 323.
[11] H.C. Bryant, I. Colbeck, A solar pond for London?, Solar Energy 19 (1977) 321.
[12] E. Leonardi, M. Rosa-Clot, Solar desalinators: an ecological and economic project to overcome the water shortage in Sardinia, CRS4 Technical Report, CRS4-TECH-REP 01/38.
[13] Numerical Recipes in FORTRAN 77: The Art of Scientific Computing, Cambridge University Press, 1992, pp. 838–842. ISBN 0-521-43064-X.
[14] E. Anderson, Z. Bai, C. Bischof, S. Blackford, J. Demmel, J. Dongarra, J. Du Croz, A. Greenbaum, S. Hammarling, A. McKenney, D. Sorensen, LAPACK Users' Guide, 3rd

Ed., Society for Industrial and Applied Mathematics, Philadelphia, PA, 1999. ISBN 0-89871-447-8.

[15] S.C. McCutcheon, J.L. Martin, T.O. Barnwell Jr., Water Quality in Maidment in Handbook of Hydrology, McGraw-Hill, New York, NY, 1993, p. 11.3.

[16] H. Tabor, Z. Weinberger, Non-convecting solar ponds, in: F. Kreith (Ed.), Solar Energy Handbook, McGraw-Hill, New York, 1981 (Chapter 10).

[17] S.G. Schlad, The dynamics of a salt gradient solar pond, Ph.D. Thesis, The University of Western Australia, 1985.